



Mono- and disubstitution reactions of gyroscope like complexes derived from Cl–Pt–Cl rotators within cage like dibridgehead diphosphine ligands



Deeb Taher ^{a,1}, Agnieszka J. Nawara-Hultzsch ^b, Nattamai Bhuvanesh ^a, Frank Hampel ^b, John A. Gladysz ^{a,*}

^a Department of Chemistry, Texas A&M University, PO Box 30012, College Station, TX 77842-3012, USA

^b Institut für Organische Chemie and Interdisciplinary Center for Molecular Materials, Friedrich-Alexander-Universität Erlangen-Nürnberg, Henkestraße 42, 91054 Erlangen, Germany

ARTICLE INFO

Article history:

Received 4 February 2016

Received in revised form

18 March 2016

Accepted 20 March 2016

Available online 23 March 2016

Special issue dedicated to Prof. Heinrich Lang: "to a superb mentor of one author (D.T.), and a great friend of another (J.A.G.)"

Keywords:

Platinum

Selenium

Gyroscope

Substitution

Crystal structure

ABSTRACT

Reaction of the gyroscope like complex *trans*-Pt(Cl)₂(P((CH₂)₁₄)₃P) (*trans*-**1c**) and *p*-tolSeSiMe₃ (3.8 equiv, 85 °C, melt) gives the disubstitution product *trans*-Pt(*Se-p-tol*)₂(P((CH₂)₁₄)₃P) (*trans*-**3c**, 63%) and ClSiMe₃. Attempts to access a monochloride complex via monosubstitution were unsuccessful. However, when *trans*-Pt(Ph)₂(P((CH₂)_n)₃P) (*trans*-**2**; *n* = **c**/14, **e**/18) and HCl (1.0 equiv; generated from CH₃COCl and excess CH₃OH) are reacted, the monochloride complexes *trans*-Pt(Cl)(Ph)(P((CH₂)_n)₃P) (*trans*-**4c,e**, 93–96%) are obtained. These feature dipolar rotators, a common design element in approaches to molecular gyroscopes. The crystal structures of *trans*-**3c** and *trans*-**4c** are determined, and the radii of the rotators and other geometrical features analyzed, especially with regard to the facility of PtL₂ rotation.

© 2016 Elsevier B.V. All rights reserved.

1. Introduction

In previous studies, we have developed a rich chemistry associated with the platinum dichloride complexes *trans*-Pt(Cl)₂(P((CH₂)_n)₃P) (*trans*-**1**; *n* = **c**/14, **d**/16, **e**/18) shown in Scheme 1 [1,2], which feature cage like, triply *trans* spanning dibridgehead diphosphine ligands. A number of related diphosphine complexes with trigonal bipyramidal and octahedral coordination geometries have also been synthesized [3]. These families of compounds have been termed "gyroscope like", and when the ligands attached to the metals are sufficiently small, rapid rotation occurs within the diphosphine cage. Hence, the PtCl₂ or ML₂ moieties are commonly referred to as rotators. Interestingly, all of the physics associated with macroscopic gyroscopes remains unaltered

at the molecular level [4].

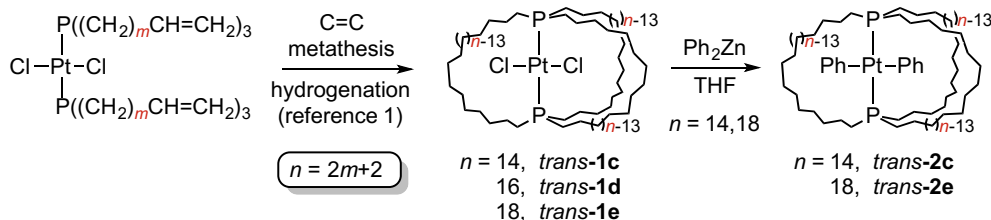
In the interest of fine tuning the attendant rotational barriers, various substitution reactions of the ML₂ cores have been developed. For example, the chloride ligands in **1c–e** can be displaced by a variety of halide and pseudohalide nucleophiles, as well as the phenyl moieties of ZnPh₂ to give *trans*-Pt(Ph)₂(P((CH₂)_n)₃P) (*trans*-**2c,e**; 61–90%) [1,2]. Rotation of the PtCl₂ moieties within the diphosphine cages in **1c–e** is rapid on the NMR time scale, even at –90 °C, as evidenced by a single set of *n*/2 CH₂ ¹³C signals [1]. In contrast, with the diphenyl complex *trans*-**2c**, rotation of the PtPh₂ moiety is slow, as evidenced by two sets of *n*/2 CH₂ ¹³C signals (ca. 2:1 area ratios). However, when the methylene chains are lengthened, such as in the higher homolog *trans*-**2e**, PtPh₂ rotation readily occurs.

Interestingly, large excesses of certain types of nucleophiles, such as acetylide, cyanide, or related –C≡X species, displace the dibridgehead diphosphine from platinum [1,2]. In some cases, salts of the platinum dianion [Pt(C≡X)₄]²⁻ have been isolated [2]. Adducts with Rh(CO)(Cl) rotators can be similarly excised with excess

* Corresponding author.

E-mail address: gladysz@mail.chem.tamu.edu (J.A. Gladysz).

¹ Current address: Chemistry Department, The University of Jordan, Amman 11942, Jordan.



Scheme 1. Syntheses and substitution reaction of the gyroscope like Cl–Pt–Cl complexes **trans-1c,e**.

PM₃ [3f]. Other types of substitution reactions (below) are believed to involve initial electron transfer [3g].

Against this backdrop, we have sought to expand the palette of chloride ligand substitution reactions applicable to *trans*-**1c–e** or their derivatives. One goal has been to apply a greater range of heteronucleophiles. Another has been to develop routes to monosubstitution products. An incentive for the latter involves potential applications of complexes possessing unsymmetrically substituted or “dipolar” rotators, X–Pt–X'. Rotation of the PtCl₂ moieties in *trans*-**1c–e** is Brownian, meaning that clockwise and counterclockwise directions are equally probable. However, dipolar rotators can, in principle, be (1) oriented in a static electric field, and (2) induced to spin unidirectionally by a rotating electric field of appropriate frequency [4,5]. The latter would constitute a functional molecular gyroscope, which has been an ongoing quest in several research groups [6,7].

2. Results

A few sulfur substituted gyroscope like complexes have been prepared, although in some cases workups have proved problematic [1,8]. Selenium analogs would provide a larger steric footprint and perhaps enhanced crystallinity. A variety of alkyl and aryl selenium nucleophiles have been shown to displace transition metal halides [9,10]. Among these, trimethylsilylated species have proven to be convenient and effective [9]. Since only a volatile trimethylsilyl halide coproduct is generated, workups should be facilitated.

Thus, as shown in **Scheme 2**, *trans*-**1c** and the easily prepared *p*-tolylselenium compound *p*-tolSeSiMe₃ (3.8 equiv) [11] were combined in THF at room temperature. The sample was periodically monitored by ³¹P NMR. After 18 h, the sample was warmed to 50 °C. After an additional 16 h, no reaction had occurred. Thus, *trans*-**1c**

and *p*-tolSeSiMe₃ were combined as solids, and the sample transferred to a 85 °C oil bath. The sample melted, giving a free flowing yellow liquid. Workup afforded the target complex *trans*-Pt(*Se-p-tol*)₂(P((CH₂)₁₄)₃P) (*trans*-**3c**) in 63% yield as an air stable polycrystalline solid.

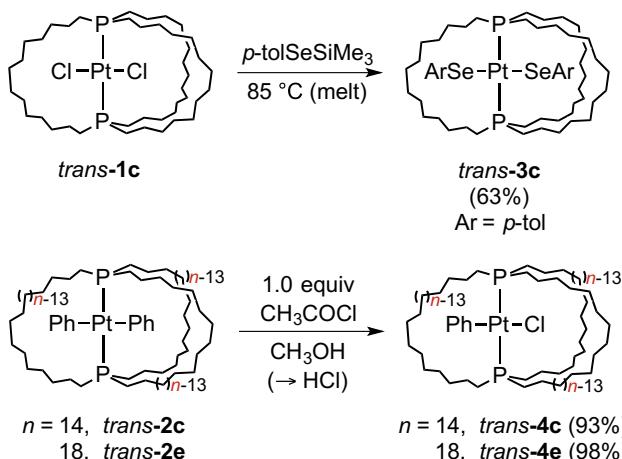
Complex *trans*-**3c** was characterized by NMR (¹H, ¹³C, ³¹P, ¹⁹⁵Pt), mass spectrometry, and microanalysis, as summarized in the experimental section. The mass spectrum showed the expected molecular ion. The ¹³C NMR spectrum exhibited *n* (14) as opposed to *n*/2 (7) CH₂ signals, indicating two inequivalent methylene chains (2:1). Thus, Pt(*Se-p-tol*)₂ rotation through the seventeen membered macrocycles must be slow on the NMR time scale or blocked completely, analogous to the situation with *trans*-**2c** noted above. As seen with **1c**, the PCH₂CH₂CH₂ signals were virtual triplets; other NMR features were routine.

Numerous attempts to develop conditions that would give a monosubstitution product with a dipolar Cl–Pt–Se–*p*-tol rotator were unsuccessful. Thus, an alternative desymmetrization approach involving electrophilic agents was considered. It has previously been shown that dialkyl and diaryl platinum(II) complexes can be selectively converted to monoalkyl or monoaryl platinum monochloride complexes when treated with HCl [12]. The electron withdrawing chloride ligand in the initial product renders it less basic (nucleophilic) than the precursor. This retards further conversion of the monochloride complex to a dichloride complex.

Thus, as shown in **Scheme 2**, CH₂Cl₂ solutions of *trans*-**2c,e** were treated with HCl (1.0 equiv). In practice, this was accomplished by adding a stoichiometric amount of the acid chloride CH₃COCl and an excess of CH₃OH. After brief intervals, ³¹P NMR spectra showed very high conversions to a single new product. Workups gave the target monochloride complexes *trans*-Pt(Cl)(Ph)(P((CH₂)_n)₃P) (*trans*-**4**; *n* = **c**/14, **e**/18) as cream colored powders in 95–98% yields. These showed no decomposition when stored in air over an extended period of time.

Complexes *trans*-**4c,e** were characterized analogously to *trans*-**3c**. Most features were unexceptional. Interestingly, both showed a single set of *n*/2 CH₂ ¹³C NMR signals. Thus, the diphenyl complex *trans*-**2c** and the monophenyl monochloride complex *trans*-**4c** exhibit different limits with respect to PtPh₂ or PtClPh rotation, a dichotomy that is analyzed in the discussion section. An attempt to effect a conceptually similar desymmetrization of *trans*-**3c** by reaction with CH₃COCl (1.0 equiv) did not lead to tractable products.

Single crystals of *trans*-**3c** and *trans*-**4c** could be obtained as described in the experimental section. The crystal structures were determined as summarized in **Table 1** and the experimental section. Thermal ellipsoid diagrams and key metrical parameters are provided in **Figs. 1 and 2**. For both structures, the angles defined by the least squares planes of the aryl rings and the P–Pt–P vector were calculated. In *trans*-**3c**, the tolyl groups were skewed (45.08°, 48.84°), whereas in *trans*-**4c** the phenyl group was nearly perpendicular (85.55°). The crystal structures of *trans*-**2c,e** exhibited analogous phenyl ring conformations. The other metrical parameters associated with the new complexes were routine, resembling



Scheme 2. New substitution chemistry of gyroscope like PtCl₂ and PtPh₂ complexes.

Table 1
Summary of crystallographic data.

Compound	<i>trans</i> -3c	<i>trans</i> -4c
Molecular formula	C ₅₆ H ₉₈ PtSe ₂	C ₄₈ H ₈₉ Cl ₂ Pt
Molecular weight	1186.29	958.67
Temp. of collection, K	150.15	173(2)
Wavelength [Å]	0.71073	0.71073
Diffractometer	BRUKER APEX 2	Nonius Kappa CCD
Crystal system	triclinic	monoclinic
Space group	P-1	P2 ₁
Unit cell dimensions:		
<i>a</i> [Å]	14.3291(17)	13.9974(2)
<i>b</i> [Å]	15.3338(18)	13.8028(3)
<i>c</i> [Å]	15.7555(19)	14.1122(3)
α [°]	65.4630(10)	90
β [°]	70.5210(10)	113.810(1)
γ [°]	67.7030(10)	90
<i>V</i> [Å ³]	2849.4(6)	2494.47(8)
<i>Z</i>	2	2
D_c [Mg/m ⁻³]	1.383	1.276
μ [mm ⁻¹]	3.829	2.959
Crystal dimensions, mm	0.07 × 0.07 × 0.06	0.20 × 0.20 × 0.20
Θ range [°]	1.571 ≤ Θ ≤ 27.437	2.16 ≤ Θ ≤ 27.53
Range/indices (<i>h,k,l</i>)	-17,18; -17,19; 0,20	-18,18; -17,17; -18,18
No. of reflections	12583	11376
No. of unique data	12583	11376
No. of observed data	10769 [<i>I</i> > 2 σ (<i>I</i>)]	10155 [<i>I</i> > 2 σ (<i>I</i>)]
No. refined parameters	553	372
R_{int}	0.0265	0.000
<i>R</i> indices [<i>I</i> > 2 σ (<i>I</i>)]	R_1 = 0.0327 wR_2 = 0.0731	R_1 = 0.0393 wR_2 = 0.0977
<i>R</i> indices (all data)	R_1 = 0.0433 wR_2 = 0.0776	R_1 = 0.0467 wR_2 = 0.1019
Goodness of fit	1.005	1.054
Largest diff. peak, hole [eÅ ⁻³]	1.071/-1.794	2.559/-1.035

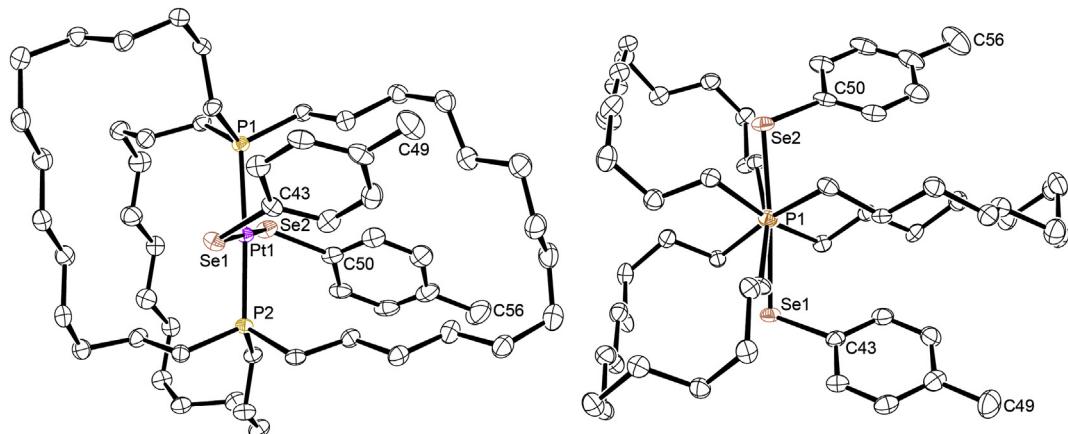


Fig. 1. Thermal ellipsoid plots of the molecular structure of *trans*-3c (50% probability level). Key interatomic distances (Å) and angles (°): Pt1–P1 2.3168(9), Pt1–P2 2.3207(9), Pt1–Se1 2.4684(4), Pt1–Se2 2.4650(5), Pt1–C49 7.394, Pt1–C56 7.368, P1–Pt1–P2 176.59(3), Se1–Pt1–Se2 176.012(14), P1–Pt1–Se1 93.99(2), P1–Pt1–Se2 86.04(2), P2–Pt1–Se1 85.92(2), P2–Pt1–Se2 93.81(2), C43–Se1–Pt1 105.90(10), C50–Se2–Pt1 105.75(11).

those found in related species earlier. For example, the Pt–Se–C angles (105.90(10)°–105.75(11)°) were near the average of those in six other platinum(II) complexes with two Pt–Se–C linkages (107.6°) [10a].

3. Discussion

The substitution reactions described above allow access to new types of platinum gyroscope like complexes and can presumably be extended to other metal fragments. Only a few methods have so far been developed by which a dipole moment can be introduced on a rotator that lacks one. In other cases, the

ring closing metatheses in **Scheme 1** are carried out on educts where the ML_y unit already has a dipole moment, such as Rh(CO)(Cl) or Re(CO)₃(Cl) [3c,d]. Another type of substitution reaction that has been used to desymmetrize a nonpolar rotator is shown in **Scheme 3** [3a,h]. This is believed to involve initial electron transfer from iron to NO⁺, generating an intermediate radical cation.

The conformations of the rotators in **Figs. 1 and 2** closely approximate those that would be expected in the ground states, as depicted in I in **Fig. 3**. All rotators are characterized by a radius. That of the PtCl₂ moiety in *trans*-1c is the sum of the platinum-chloride distance and the van der Waals radius of chlorine (1.75 Å) [13], or

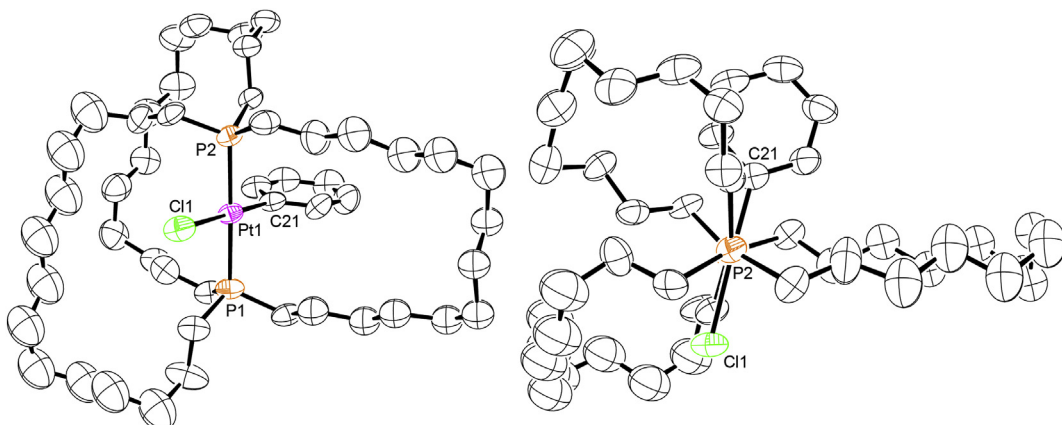
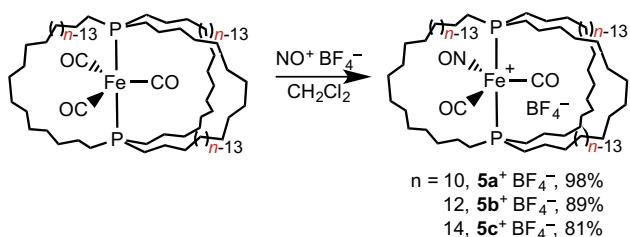


Fig. 2. Thermal ellipsoid plots of the dominant conformation of the molecular structure of *trans*-4c (50% probability level). Key interatomic distances (Å) and angles (°): Pt–P1 2.3025(15), Pt–P2 2.2968(14), Pt–C11 2.3871(15), Pt–C21 2.006(6), Pt–H_{para} 5.781, P1–Pt–P2 176.86(5), Cl1–Pt–C21 178.62(19).



Scheme 3. Other substitution reactions of gyroscope like complexes leading to dipolar rotators.

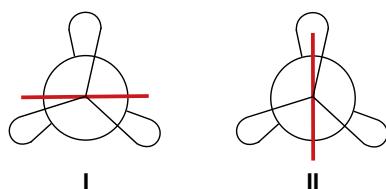


Fig. 3. Newman type projections of the energy minima (I) and maxima (II) associated with rotation of the rotator in square planar gyroscope like complexes.

approximately 4.05–4.06 Å [1]. As analyzed previously, the radius of a PtPh₂ moiety is ca. 7.07–7.08 Å [1]. The radius of the rotator in *trans*-3c was taken as the sum of the distance from platinum to the *p*-methyl groups (7.37–7.39 Å), plus the van der Waals radius of an sp³ hybridized carbon atom (1.70 Å) [13], or 9.07–9.09 Å.

The crystal structures of a variety of complexes of the formula $\text{trans-Pt}(\text{L})_2(\text{P}((\text{CH}_2)_{14})_3\text{P})$ have been determined [1]. These feature seventeen membered macrocycles like the new structures in Figs. 1 and 2. It is a simple matter to compute the distances from the metal to the two carbon atoms of each macrocycle closest to the plane of the rotators, and/or the most distant carbon atoms. As diagrammed elsewhere [1b,3g,h], the van der Waals radius of the carbon atom is then subtracted to give an estimate of the “horizontal clearance” for the rotators. Naturally, as evident in Fig. 1, the conformations of the macrocycles differ, resulting in different clearances. Often the minimum value is taken as the starting point for analysis, but other treatments, such as average values, can be considered. In the case of *trans*-1c, the values range from 3.76 Å to 5.75 Å. Those for *trans*-2c vary from 3.51 Å to 6.09 Å. In the case of *trans*-2e, which features twentyone membered macrocycles, the values range from 4.22 Å to 8.79 Å [1b].

In square planar gyroscope like complexes, the transition states for rotation would normally involve passage of one ligand of a rotator through a single macrocycle, as shown in **II**. There will be six such maxima as the rotator passes through 360°. With respect to selenium substituted *trans*-3c, it is evident that the radius of the rotator greatly exceeds the maximum extension or clearance possible with seventeen membered macrocycles (9.07–9.09 Å vs. ca. 6.09 Å). With respect to the previously studied diphenyl complex *trans*-2e, the facile PtPh₂ rotation needs to be viewed in the context of the maximum extension or clearance possible in a twentyone membered macrocycle (8.79 Å vs. 7.07–7.08 Å radius). The macrocycles do not remain rigid as the PtPh₂ moiety rotates; rather, they undergo correlated conformational changes, which would enable the macrocycle thorough which the phenyl group is passing (see **II**) to be maximally extended.

The surprise regarding the new compound *trans*-4c is that PtClPh rotation through the seventeen membered ring is rapid on the NMR time scale at room temperature, but PtPh₂ rotation in *trans*-2c is not. The horizontal clearances imposed by the methylene chains in crystalline *trans*-4c (3.17 Å to 6.28 Å) [14] are similar to those in *trans*-2c (3.51 Å to 6.09 Å). Hence, the barrier is not a strict function of the radius of the rotator, which is the same in both cases. In this context, NMR spectra of *trans*-2c further indicate that rotation about the Pt–Ph bonds is restricted, as evidenced by two *ortho* and two *meta* ¹³C signals. Only one set of signals is observed with *trans*-4c. Thus, there appears to be more extensive interactions of the phenyl rings with the cage like diphosphine in *trans*-2c. In any case, with *trans*-4c a rotator of radius 7.02–7.03 Å is able to pass through macrocycles for which the maximum solid state clearance is 6.28 Å [14].

In summary, this study has expanded the toolbox of substitution reactions applicable to gyroscope like complexes, and provided further data and insight regarding their dynamic properties. Future efforts will extend these themes to additional coordination geometries [3g], including syntheses of other types of complexes with dipolar rotators, and minimization of the rotational barriers therein.

4. Experimental section

General. Reactions were conducted under dry inert atmospheres using solvents and materials detailed in the previous full paper [1b]. Instruments employed were identical with those listed in the previous full paper [1b].

trans-Pt(Se-*p*-tol)₂(P((CH₂)₁₄)₃P) (*trans*-3c) A Schlenk tube was charged with *trans*-Pt(Cl)₂(P((CH₂)₁₄)₃P) (*trans*-1c [1b]; 0.100 g,

0.109 mmol) and *p*-tolSeSiMe₃ (0.100 g, 0.411 mmol) [9], and was partially evacuated. The tube was placed in an 85 °C oil bath, whereupon the solids melted to yield a yellow, free-flowing liquid. After 18 h, the mixture had become a yellow solid and was cooled to room temperature. Any residual Me₃SiCl was removed in vacuo, and the residue was washed with pentane. Crystallization from pentane/dichloromethane (3 mL, 1:1 v/v) gave the solvate *trans*-**3c**·0.33CH₂Cl₂ as a yellow, air stable polycrystalline solid (0.084 g, 0.071 mmol, 65%), dec. pt. 125 °C (yellow solid to orange solid). Anal. Calcd for C₅₆H₉₈Pt₂Se₂·0.33CH₂Cl₂: C, 55.70; H, 8.19; found: C, 55.60; H, 8.47. MS [15a]: 1186.5724 ([M]⁺, 14%), 1015.5921 ([M-SeC₆H₄CH₃]⁺, 9%).

NMR (CDCl₃, δ (ppm)) [16]: ¹H (500 MHz) 7.53 (d, $^3J_{HH}$ = 10 Hz, 4H of 2C₆H₄), 6.86 (d, $^3J_{HH}$ = 10 Hz, 4H of 2C₆H₄), 5.30 (s, 0.67H, 0.33CH₂Cl₂), 2.52–2.46 (m, 4H, PCH₂), 2.25 (s, 6H, CH₃), 1.65–1.78 (m, 8H, CH₂), 1.51–1.20 (m, 70H, CH₂), 0.89–0.86 (m, 2H, CH₂); ¹³C {¹H} (126 MHz) C₆H₄ at 134.9 (s, J_{CSe} = 30.0 Hz) [17], 133.3, 133.1, and 128.8 (3 \times s); 31.0 (virtual t [18], J_{CP} = 7.8 Hz, PCH₂CH₂CH₂), 29.6 (virtual t [18], J_{CP} = 6.6 Hz, PCH₂CH₂CH₂), 29.0 (s, CH₃), 28.9 (s, CH₂), 28.6 (s, CH₂), 28.3 (s, CH₂), 28.0 (s, CH₂), 27.9 (s, CH₂), 26.8 (s, CH₂), 26.7 (s, CH₂), 25.9 (s, PCH₂CH₂), 25.5 (virtual t [18], J_{CP} = 17.0 Hz, PCH₂), 22.7 (s, PCH₂CH₂), 21.2 (s, CH₂), 20.9 (virtual t [18], J_{CP} = 17.1 Hz, PCH₂); ³¹P{¹H} (202 MHz) 1.4 (s, $^1J_{PPT}$ = 2516 Hz), ¹⁹⁵Pt{¹H} (202 MHz) –4879.7 (s, $^1J_{PtP}$ = 2509 Hz) [19,20].

trans-Pt(Cl)(Ph)(P((CH₂)₁₄)₃P) (*trans*-**4c**) A 5 mm NMR tube was charged with *trans*-Pt(Ph)₂(P((CH₂)₁₄)₃P) (*trans*-**2c** [1]; 0.0378 g, 0.0378 mmol), CH₂Cl₂ (0.40 mL), CH₃OH (0.10 mL), and CH₃COCl (0.0033 mL, 0.0378 mmol). After 5 min, a ³¹P{¹H} NMR spectrum showed >99% conversion. The solvent was removed by oil pump vacuum, and benzene was added to the residue. The suspension was filtered through a pipette packed with silica gel, which was rinsed with benzene. The solvent was removed from the filtrate by freeze pump drying to give *trans*-**4c** as a cream colored powder (0.0339 g, 0.0354 mmol, 93%). DSC (T_i/T_e/T_p/T_c/T_f) [21]: 142.0/190.6/196.7/198.3/206.8 °C (endotherm). TGA: onset of mass loss, 254 °C. Anal. Calcd. for C₄₈H₈₉Cl₂Pt: C, 60.14; H, 9.36. Found: C, 59.85; H, 9.61. IR (cm^{−1}, powder film): 2922 (s), 2853 (s), 1571 (w), 1455 (m), 1262 (w), 1100 (m), 1023 (w), 799 (m), 733 (s), 702 (s). MS [15b]: 923 ([M–Cl]⁺, 70%).

NMR (δ (ppm), CDCl₃) [16]: ¹H (400 MHz) 7.23 (d, $^1J_{HH}$ = 7.4 Hz, 2H, o-Ph), 6.89 (apparent t, $^1J_{HH}$ = 7.0 Hz, 2H, m-Ph), 6.81 (t, $^1J_{HH}$ = 7.1 Hz, 1H, p-Ph), 1.72–1.62 (br m, 12H, PCH₂), 1.55–1.46 (br m, 12H, PCH₂CH₂), 1.45–1.36 (br m, 12H, PCH₂CH₂CH₂), 1.33–1.25 (br m, 48H, remaining CH₂); ¹³C{¹H} (100 MHz) 138.2 (s, i-Ph) [22], 137.4 (s, o-Ph), 127.3 (s, m-Ph), 121.6 (s, p-Ph), 29.7 (virtual t [18], J_{CP} = 6.8 Hz, PCH₂CH₂CH₂), 29.2 (virtual t [18], J_{CP} = 6.7 Hz, PCH₂CH₂CH₂), 28.6 (s, CH₂), 28.2 (s, CH₂), 27.3 (s, CH₂), 26.7 (s, CH₂), 26.6 (s, CH₂), 26.3 (s, CH₂), 23.2 (s, CH₂), 21.7 (virtual t [18], J_{CP} = 15.7 Hz, PCH₂), 19.3 (virtual t [18], J_{CP} = 16.0 Hz, PCH₂); ³¹P{¹H} (162 MHz) 7.8 (s, $^1J_{PPT}$ = 2798 Hz) [20].

trans-Pt(Cl)(Ph)(P((CH₂)₁₈)₃P) (*trans*-**4e**) A 5 mm NMR tube was charged with *trans*-Pt(Ph)₂(P((CH₂)₁₈)₃P) (*trans*-**2e** [1]; 0.0159 g, 0.0136 mmol), CH₂Cl₂/CH₃OH (0.75 mL, 2:1 v/v), and CH₃COCl (0.0117 mL, 0.0136 mmol). After 1 h, a ³¹P{¹H} NMR spectrum showed >99% conversion. The solvent was removed by oil pump vacuum, and benzene was added to the residue. The suspension was filtered through a pipette packed with glass fibers. The pipette was rinsed with benzene. The solvent was removed by freeze pump drying to give *trans*-**4e** as a cream-colored powder (0.0142 g, 0.0121 mmol, 98%). DSC: (T_i/T_e/T_p/T_c/T_f) [21]: 31.1/31.1/33.6/36.8/37.2 (endotherm), 49.2/75.9/81.3/83.6/86.5 (endotherm), 87.1/94.4/99.3/102.5/105.0 (endotherm). TGA: onset of mass loss, 190 °C. Anal. Calcd. for C₆₀H₁₁₃Cl₂Pt: C, 63.94; H, 10.11. Found: C, 64.14; H,

10.23. IR (cm^{−1}, powder film): 2922 (s), 2853 (s), 1571 (w), 1463 (m), 1370 (w), 1262 (w), 1100 (m), 1027 (m), 795 (m), 702 (m). MS [15b]: 1091 ([M–Cl]⁺, 80%).

NMR (δ (ppm), CDCl₃) [16]: ¹H (400 MHz) 7.23 (d, $^1J_{HH}$ = 7.4 Hz, 2H, o-Ph), 6.87 (apparent t, $^1J_{HH}$ = 6.7 Hz, 2H, m-Ph), 6.81 (t, $^1J_{HH}$ = 7.2 Hz, 1H, p-Ph), 1.50–1.31 (br m, 30H, CH₂), 1.31–1.04 (br m, 78H, CH₂); ¹³C{¹H} [23] (100 MHz) 137.2 (s, o-Ph), 127.6 (s, m-Ph), 121.5 (s, p-Ph), 30.5 (virtual t [18], $^3J_{CP}$ = 6.2 Hz, PCH₂CH₂CH₂), 28.5 (s, CH₂), 28.4 (s, CH₂), 28.32 (s, CH₂), 28.29 (s, CH₂), 28.0 (s, CH₂), 27.8 (s, CH₂), 23.4 (s, PCH₂CH₂), 21.2 (virtual t [18], $^3J_{CP}$ = 15.8 Hz, PCH₂); ³¹P{¹H} (162 MHz) 7.1 (s, $^1J_{PPT}$ = 2774 Hz) [20].

Crystallography. **A.** Light yellow plates of *trans*-**3c** were obtained by the slow evaporation of a CHCl₃/CH₂Cl₂ solution (1:1 v/v, room temperature). Data were collected on a two component twin as outlined in Table 1. Cell parameters were determined from 60 data frames taken at 0.5° widths. Integrated intensity information for each reflection (for both twins) was obtained by reduction of the data frames with the program APEX2 [24]. Data were corrected for Lorentz, polarization, and crystal decay effects. The program TWI-NABS [25] was used to correct for absorption. Systematic reflection conditions and statistical tests of the data suggested the space group *P*-1. The structure was solved by direct methods using SHELXTL (XS) [26]. Hydrogen atoms were placed in idealized positions and refined using a riding model. Non-hydrogen atoms were refined with anisotropic thermal parameters. The absence of additional symmetry and voids were confirmed using PLATON (ADDSYM) [27]. The structure was refined (weighted least squares refinement on F^2) to convergence [26,28]. **B.** CH₂Cl₂ was added to a pentane suspension of *trans*-**4c** until the sample became homogeneous. The mixture was allowed to slowly concentrate to ca. 50% of the original volume (room temperature). After one day, colorless cubes of *trans*-**4c** had formed. Data were collected as outlined in Table 1. Cell parameters were obtained from 10 frames using a 10° scan and refined with 5952 reflections. Lorentz, polarization, and absorption corrections were applied [29]. The space group was determined from systematic absences and subsequent least-squares refinement. The structure was solved by direct methods. The parameters were refined with all data by full-matrix-least-squares on F^2 using SHELXL-97 [26]. Non-hydrogen atoms were refined with anisotropic thermal parameters. The hydrogen atoms were fixed in idealized positions using a riding model. Scattering factors were taken from the literature [30]. Three methylene carbon atoms were disordered and were refined to a 67:33 occupancy ratio.

Acknowledgment

The authors thank the U.S. National Science Foundation (CHE-1153085), the Fulbright Foundation (D.T.), and the University of Jordan (D.T.) for support, and Dr. Tobias Fiedler, Ms. Georgette Lang, and Mr. Alex Estrada for technical assistance.

Supplementary material

CCDC 1450263 and 955809 contain the supplementary crystallographic data for *trans*-**3a** and *trans*-**4a**. These data can be obtained free of charge from The Cambridge Crystallographic Data Centre via www.ccdc.cam.ac.uk/data_request/cif.

References

- [a] A.J. Nawara, T. Shima, F. Hampel, J.A. Gladysz, J. Am. Chem. Soc. 128 (2006) 4962–4963;
- [b] A.J. Nawara-Hultsch, M. Stollenz, M. Barbasiewicz, S. Szafert, T. Lis, F. Hampel, N. Bhuvanesh, J.A. Gladysz, Chem. Eur. J. 20 (2014) 4617–4637.
- [2] M. Stollenz, M. Barbasiewicz, A.J. Nawara-Hultsch, T. Fiedler, R.M. Laddusaw,

N. Bhuvanesh, J.A. Gladysz, *Angew. Chem. Int. Ed.* **50** (2011) 6647–6651; *Angew. Chem.* **2011**, *123*, 6777–6781.

[3] (a) T. Shima, F. Hampel, J.A. Gladysz, *Angew. Chem. Int. Ed.* **43** (2004) 5537–5540. *Angew. Chem.* **2004**, *116*, 5653–5656; (b) L. Wang, F. Hampel, J.A. Gladysz, *Angew. Chem. Int. Ed. Engl.* **45** (2006) 4372–4375. *Angew. Chem.* **2006**, *118*, 4479–4482; (c) L. Wang, T. Shima, F. Hampel, J.A. Gladysz, *Chem. Commun.* (2006) 4075–4077; (d) G.D. Hess, F. Hampel, J.A. Gladysz, *Organometallics* **26** (2007) 5129–5131; (e) K. Skopek, J.A. Gladysz, *J. Organomet. Chem.* **693** (2008) 857–866; (f) A.L. Estrada, T. Jia, N. Bhuvanesh, J. Blümel, J.A. Gladysz, *Eur. J. Inorg. Chem.* (2015) 5318–5321; (g) Fiedler, T.; Bhuvanesh, N.; Hampel, F.; Reibenspies, J. H.; Gladysz, J. A. *Dalton Trans.*, **45**, in press; DOI: 10.1039/c6dt00692b; (h) G.M. Lang, T. Shima, L. Wang, K. Cluff, K. Skopek, F. Hampel, J. Blümel, J.A. Gladysz, *J. Am. Chem. Soc.* (submitted for publication).

[4] G.S. Kottas, L.I. Clarke, D. Horinek, J. Michl, *Chem. Rev.* **105** (2005) 1281–1376.

[5] (a) V. Bermudez, N. Capron, T. Gase, F.G. Gatti, F. Kajzar, D.A. Leigh, F. Zerbetto, S. Zhang, *Nature* **406** (2000) 608–611; (b) R.D. Horansky, L.I. Clarke, J.C. Price, T.-A.V. Khuong, P.D. Jarowski, M.A. Garcia-Garibay, *Phys. Rev. B* **72** (2005), 014302-1 to 014302-5; (c) R.D. Horansky, L.I. Clarke, E.B. Winston, J.C. Price, S.D. Karlen, P.D. Jarowski, R. Santillan, M.A. Garcia-Garibay, *Phys. Rev. B* **74** (2006), 054306-1 to 054306-12; (d) P. Dhar, C.D. Swayne, T.M. Fischer, T. Kline, A. Sen, *Nano Lett.* **7** (2007) 1010–1012; (e) J.J. Arcenegui, P. García-Sánchez, H. Morgan, A. Ramos, *Phys. Rev. E* **88** (2013), 033025-1 to 033025-8.

[6] (a) T.-A.V. Khuong, J.E. Nuñez, C.E. Godinez, M.A. Garcia-Garibay, *Acc. Chem. Res.* **39** (2006) 413–422; (b) C.S. Vogelsberg, M.A. Garcia-Garibay, *Chem. Soc. Rev.* **41** (2012) 1892–1910; (c) P. Commins, M.A. Garcia-Garibay, *J. Org. Chem.* **79** (2014) 1611–1619.

[7] (a) Y. Nishiyama, Y. Inagaki, K. Yamaguchi, W. Setaka, *J. Org. Chem.* **80** (2015) 9959–9966 and references therein; (b) E. Prack, C.A. O’Keefe, J.K. Moore, A. Lai, A.J. Lough, P.M. Macdonald, M.S. Conradi, R.W. Schurko, U. Fekl, *J. Am. Chem. Soc.* **137** (2015) 13464–13467.

[8] G.D.U. Heß, doctoral dissertation, Universität Erlangen-Nürnberg, 2010; Scheme 2.6 and pp 77–78.

[9] D. Taher, N.J. Taylor, J.F. Corrigan, *Can. J. Chem.* **87** (2009) 380–385.

[10] (a) M.S. Hannu-Kuure, J. Komulainen, R. Oilunkaniemi, R.S. Laitinen, R. Suontamo, M. Ahlgren, *J. Organomet. Chem.* **666** (2003) 111–120; (b) D. Taher, *Trans. Met. Chem.* **34** (2009) 641–645.

[11] K. Praefcke, C. Weichsel, *Synthesis* **3** (1980), 216–216.

[12] (a) H.C. Clark, L.E. Manzer, *J. Organomet. Chem.* **59** (1973) 411–428; (b) T.B. Peters, Q. Zheng, J. Stahl, J.C. Bohling, A.M. Arif, F. Hampel, J.A. Gladysz, *J. Organomet. Chem.* **641** (2002) 53–61.

[13] A. Bondi, *J. Phys. Chem.* **68** (1964) 441–451.

[14] The distances from platinum to the two carbon atoms of each macrocycle closest to the plane of the rotator in *trans*-**4c** are 7.564/7.642 Å, 4.867/5.552 Å, and 5.277/5.640 Å. When the van der Waals radius of carbon is subtracted from the longest and shortest distances, limiting clearances of 3.17 Å and 6.28 Å are obtained.

[15] *m/z* (relative intensity, %); the most intense peak of isotope envelope is given. (a) MALDI+; (b) FAB, 3-NBA.

[16] The ¹H and ¹³C NMR assignments were made by analogy to those in reference **1b**, which were established by 2D NMR experiments.

[17] This coupling represents a satellite (*d*, ⁷⁷Se = 7.6%) and is not reflected in the peak multiplicity given.

[18] W.H. Hersh, *J. Chem. Educ.* **74** (1997) 1485–1489 (The *J* values given represent the apparent coupling between adjacent peaks of the triplet).

[19] This spectrum was referenced to a D₂O solution of the external standard K₂PtCl₆ (–1620 ppm).

[20] This coupling represents a satellite (*d*, ¹⁹⁵Pt = 33.8%) and is not reflected in the peak multiplicity given.

[21] DSC and TGA data were treated as recommended by Cammenga, H. K.; Epple, M. *Angew. Chem., Int. Ed.* **1995**, *34*, 1171–1187; *Angew. Chem.* **1995**, *107*, 1284–1301. The *T_e* values best represent the temperature of the phase transition or exotherm.

[22] The expected platinum satellite was not observed.

[23] The *i*-Ph ¹³C signal was not observed.

[24] APEX2 “Program for Data Collection on Area Detectors” BRUKER AXS Inc., 5465 East Cheryl Parkway, Madison, WI, USA 53711–55373 .

[25] G.M. Sheldrick, “TWINABS: Program for Absorption Correction of Area Detector Frames”, Bruker AXS Inc., 5465 East Cheryl Parkway, Madison, WI, USA 53711–55373.

[26] G.M. Sheldrick, *Acta Cryst. A* **64** (2008) 112–122.

[27] A.L. Spek, PLATON - a multipurpose crystallographic tool, *J. Appl. Cryst.* **36** (2003) 7–13.

[28] O.V. Dolomanov, L.J. Bourhis, R.J. Gildea, J.A.K. Howard, H. Puschmann, *J. Appl. Cryst.* **42** (2009) 339–341.

[29] (a) “Collect” Data Collection Software, Nonius B.V, 1998; (b) Z. Otwinowski, W. Minor, “Scalepack” data processing software, in: *Methods in Enzymology*, 276, 1997, pp. 307–326 (Macromolecular Crystallography, Part A); (c) CrysAlisRED and KM-4-CCD Software, Oxford Diffraction, Wroclaw, Poland, 2003.

[30] D.T. Cromer, J.T. Waber, in: J.A. Ibers, W.C. Hamilton (Eds.), *International Tables for X-ray Crystallography*, Kynoch, Birmingham, England, 1974.